ELSEVIER

Probabilistic Engineering Mechanics 16 (2001) 219–231

PROBABILISTIC ENGINEERING MECHANICS

www.elsevier.com/locate/probengmech

Bayesian time–domain approach for modal updating using ambient data

Ka-Veng Yuen[a], Lambros S. Katafygiotis[b,*]

[a]Division of Engineering and Applied Science, California Institute of Technology, Pasadena, CA, USA
[b]Department of Civil Engineering, Hong Kong University of Science and Technology, Clear Water Bay, Kowloon, Hong Kong

Abstract

The problem of identification of the modal parameters of a structural model using measured ambient response time histories is addressed. A Bayesian time–domain approach for modal updating is presented which is based on an approximation of a conditional probability expansion of the response. It allows one to obtain not only the optimal values of the updated modal parameters but also their associated uncertainties, calculated from their joint probability distribution. Calculation of the uncertainties of the identified modal parameters is very important if one plans to proceed in a subsequent step with the updating of a theoretical finite-element model based on modal estimates. The proposed approach requires only one set of response data. It is found that the updated PDF can be well approximated by a Gaussian distribution centered at the optimal parameters at which the updated PDF is maximized. Examples using simulated data are presented to illustrate the proposed method.

Keywords: Bayesian; Modal updating; Model updating; System identification; Ambient vibrations; Correlation function; Time series analysis; Modal parameters

1. Introduction

The problem of identification of the modal parameters of a linear structural model using dynamic data has received much attention over the years because of its importance in model updating, response prediction, structural control and health monitoring. Many methodologies have been formulated, in both time and frequency domain, for the case where the input excitation has been measured [1,2].

Much attention has also been devoted to the identification of modal parameters in the case where no input but only response measurements are available. In particular, a lot of effort has been devoted to the case of free vibrations or impulse response and to the case of ambient vibrations. In the former case, often time–domain methods based on ARMA models are employed, using least-squares as an integral part of their formulations. It has been found that the least-squares method yields biased estimates [3]. A number of methods have been developed to eliminate this bias, including the instrumental matrix with delayed observations method [3], the correlation fit method [4], the double least-squares method [5,6] and the total least-squares method [7]. A comprehensive comparison of such methods can be found in Ref. [8].

Ambient vibrations surveys (AVS) have also attracted much interest because they offer a means of obtaining dynamic data in an efficient manner, without requiring the set-up of special dynamic experiments which are usually costly, time consuming, and often obtrusive. In AVS, the naturally occurring vibrations of the structure (due to wind, traffic, micro-tremors) can be measured and system identification techniques can be used to identify the small-amplitude modal frequencies and modeshapes of the lower modes of the structure. The assumption usually made is that the input excitation is a broad-band stochastic process adequately modeled by white noise. Many time–domain methods were developed to tackle this problem. One example is the random decrement technique [9] which is based on curve-fitting of the estimated random decrement functions corresponding to various triggering conditions. Another example is the instrumental variable method [10]. Several methods are based on fitting directly the correlation functions using least-squares type of approaches [11]. Different ARMA-based methods have been proposed, for example, the two-stage least-squares method [12]. The prediction error method [13,14] and the subspace matrices decomposition method [15] utilize the Kalman filter [16] to obtain the modal parameters. The use of extended Kalman filter for estimating the dynamic properties of a linear multi-degree-of-freedom (MDOF) system was proposed in Refs. [17–19]. The procedure starts with a single-degree-of-freedom (SDOF) system and expands the number of degrees of freedom (DOF) one by one to efficiently identify all parameters

* Corresponding author. Tel.: +852-2358-8750; fax: +852-2358-1534.
E-mail address: lambros@ust.hk (L.S. Katafygiotis).

0266-8920/01/$ - see front matter
PII: S0266-8920(01)00004-2

using incomplete response measurements. Methods for treating nonlinear systems have also been investigated using equivalent multi-input–single-output system [20].

The results of modal identification are usually restricted to the 'optimal' estimates of the modal parameters. However, there is additional information, which is valuable for further processing, related to the uncertainty associated with the above estimates. For example, in the case where the results of the above modal identification are used to update the theoretical finite-element model of a structure, the updating procedure usually requires the minimization of a positive-definite quadratic objective function involving the differences between the theoretical and identified experimental modal parameters. The weighting matrix in this objective function must reflect the uncertainties in the values of the identified modal parameters in a way that parameters which are more uncertain are weighed less. A proper selection is to set the weighting matrix equal to the inverse of the covariance matrix of these parameters. In practice, usually this covariance matrix is estimated by calculating the statistics of the optimal estimates of the modal parameters obtained from many sets of ambient data.

Recent interest has been developed for determining the uncertainties of the modal estimates in AVS using Bayesian probabilistic approaches. In Refs. [21,22], a Bayesian probabilistic system identification framework was presented for the case of measured input. In this work, we present a Bayesian time–domain approach for modal updating using ambient data. The proposed approach allows for direct calculation of the probability density function (PDF) of the modal parameters.

In the next section, we demonstrate first with an SDOF example the computational difficulties encountered when casting the exact formulation of the Bayesian methodology for modal updating using time–domain data. We then present for the general case of linear MDOF systems a new approximate approach which overcomes these difficulties and renders this problem computationally feasible. In the last section, we demonstrate the proposed approach with numerical examples.

2. Bayesian time–domain approach

2.1. Exact SDOF formulation

Consider a SDOF oscillator with equation of motion:

$$\ddot{x} + 2\zeta\omega_0\dot{x} + \omega_0^2 x = f(t) \tag{1}$$

where ω_0 and ζ are the natural frequency and damping ratio of the oscillator, respectively, and $f(t)$ the Gaussian white noise with spectral density:

$$S_f(\omega) = S_{f0} \tag{2}$$

It is well known [23] that the response $x(t)$ is a Gaussian random process with zero mean, auto-correlation function

$$R_x(\tau) = \frac{\pi S_{f0}}{2\zeta\omega_0^3} e^{-\zeta\omega_0|\tau|}\left[\cos(\omega_{0D}\tau) + \frac{\zeta}{\sqrt{1-\zeta^2}}\sin(\omega_{0D}|\tau|)\right] \tag{3}$$

and spectral density function

$$S_x(\omega) = \frac{S_{f0}}{(\omega^2 - \omega_0^2)^2 + (2\zeta\omega\omega_0)^2} \tag{4}$$

where $\omega_{0D} = \omega_0\sqrt{1-\zeta^2}$ is the damped natural frequency of the oscillator.

Assume discrete data, with time step Δt, and let $y(k)$ denote the measured response at time $t = k\Delta t$. Also, assume that due to measurement noise and modeling error, there is a difference between the measured response $y(k)$ and the model response $x(k)$, referred to hereafter as prediction error, which can be adequately represented by a discrete white noise process n with zero mean and variance σ_n^2, that is,

$$y(k) = x(k) + n(k), \qquad k = 1, \ldots, N \tag{5}$$

where the prediction error process n satisfies:

$$E[n(m)n(p)] = \sigma_n^2\delta_{m,p} \tag{6}$$

where $\delta_{m,p}$ denotes the Kronecker delta function, which is given by:

$$\delta_{m,p} = \begin{cases} 1 & \text{if } m = p \\ 0 & \text{if } m \neq p \end{cases} \tag{7}$$

Let $\mathbf{a} = [\omega_0, \zeta, S_{f0}, \sigma_n]^T$ denote the vector of parameters to be identified. Also, let $\mathbf{Y}_{1,N}$ denote the random vector $[y(1), \ldots, y(N)]^T$, where $y(k)$, $k = 1, \ldots, N$ is given by Eq. (5). It follows that the PDF of $\mathbf{Y}_{1,N}$ for given $\mathbf{a}$ is

$$p(\mathbf{Y}_{1,N}|\ \mathbf{a}) = (2\pi)^{-N/2}|\boldsymbol{\Gamma}(\mathbf{a})|^{-1/2}\exp\left[-\tfrac{1}{2}\mathbf{Y}_{1,N}^T\boldsymbol{\Gamma}^{-1}(\mathbf{a})\mathbf{Y}_{1,N}\right] \tag{8}$$

that is, it is an N-variate Gaussian distribution with zero mean and covariance matrix $\boldsymbol{\Gamma}(\mathbf{a})$ with (m, p) element $\Gamma^{(m,p)}(\mathbf{a}) = R_x[(p-m)\Delta t|\mathbf{a}] + \sigma_n^2\delta_{m,p}$, where the auto-correlation term R_x is calculated from Eq. (3) for the given system parameters $\mathbf{a}$. In the above equation and throughout this paper, the notation $|\mathbf{A}|$ is used to denote the determinant of a matrix $\mathbf{A}$.

Herein, we are concerned with the identification of the modal parameter vector $\mathbf{a}$ given some measured data $\hat{\mathbf{Y}}_{1,N}$. Using Bayes' theorem, the updated PDF of the model parameters $\mathbf{a}$ given data $\hat{\mathbf{Y}}_{1,N}$ is given by

$$p(\mathbf{a}|\hat{\mathbf{Y}}_{1,N}) = c_1 p(\mathbf{a})p(\hat{\mathbf{Y}}_{1,N}|\mathbf{a}) \tag{9}$$

where c_1 is a normalizing constant such that the integral of the right-hand side of Eq. (9) over the domain of $\mathbf{a}$ is equal to unity. The term $p(\mathbf{a})$ in Eq. (9) denotes the prior PDF of the parameters. The term $p(\hat{\mathbf{Y}}_{1,N}|\mathbf{a})$ is the dominant term on the right-hand side of Eq. (9). It is given by Eq. (8),

substituting $\mathbf{Y}_{1,N}$ with $\hat{\mathbf{Y}}_{1,N}$, and reflects the contribution of the measured data $\hat{\mathbf{Y}}_{1,N}$ in establishing the updated (posterior) PDF of **a**. Note that the relative plausibility between two values of **a** does not depend on the normalizing constant c_1. It only depends on the relative values of the prior PDF $p(\mathbf{a})$ and the relative values of $p(\hat{\mathbf{Y}}_{1,N}|\mathbf{a})$. In order to establish the most probable value of **a**, denoted by $\hat{\mathbf{a}}$ and referred to as the 'optimal' parameters, one must maximize $p(\mathbf{a})p(\hat{\mathbf{Y}}_{1,N}|\mathbf{a})$. However, for a large number of observed data, which is usually the case in AVS, repeated evaluations of the term $p(\hat{\mathbf{Y}}_{1,N}|\mathbf{a})$ for different values of **a** becomes computationally prohibitive. This becomes obvious from Eq. (8) by noting that it requires the calculation of the inverse and the determinant of the $N \times N$ matrix $\mathbf{\Gamma}(\mathbf{a})$ which becomes very expensive for large N. Therefore, the Bayesian approach described above, based on direct use of the measured data $\hat{\mathbf{Y}}_{1,N}$, becomes practically infeasible. In the next section, we present a new approximate approach which overcomes these difficulties and renders the problem computationally feasible.

2.2. Proposed approximate MDOF formulation

Consider a system with N_d DOFs and equation of motion:

$$\mathbf{M}\ddot{\mathbf{x}} + \mathbf{C}\dot{\mathbf{x}} + \mathbf{K}\mathbf{x} = \mathbf{F}(t) \tag{10}$$

where **M**, **C** and **K** are the mass, damping and stiffness matrices of the oscillator, respectively, and $\mathbf{F}(t)$ the Gaussian white noise with spectral density matrix:

$$\mathbf{S}_F(\omega) = \mathbf{S}_{F0} \tag{11}$$

Using modal analysis, we obtain the uncoupled modal equations of motion:

$$\ddot{q}_r(t) + 2\zeta_r\omega_r\dot{q}_r(t) + \omega_r^2 q_r(t) = f_r(t), \qquad r = 1,\ldots,N_d \tag{12}$$

where $\mathbf{q}(t) = [q_1(t),\ldots,q_{N_d}(t)]^{\mathrm{T}}$ is the modal coordinate vector and $\mathbf{f}(t) = [f_1(t),\ldots,f_{N_d}(t)]^{\mathrm{T}}$ the modal forcing vector. The transformation between the original coordinates (forces) and the modal coordinates (forces) is given by

$$\mathbf{x}(t) = \mathbf{\Phi}\cdot\mathbf{q}(t) \tag{13}$$

$$\mathbf{f}(t) = (\mathbf{M}\mathbf{\Phi})^{-1}\cdot\mathbf{F}(t) \tag{14}$$

where $\mathbf{\Phi}$ is the modeshape matrix, comprised of the modeshape vectors $\phi^{(r)}$ which are assumed to be normalized such that:

$$\phi_{i_r}^{(r)} = 1, \qquad r = 1,\ldots,N_d \tag{15}$$

where i_r is a measured DOF which is not a node of the rth mode.

The spectral density matrix of the modal forcing vector $\mathbf{f}(t)$ is given by

$$\mathbf{S}_f(\omega) = \mathbf{S}_{f0} = (\mathbf{M}\mathbf{\Phi})^{-1}\mathbf{S}_{F0}(\mathbf{M}\mathbf{\Phi})^{-\mathrm{T}} \tag{16}$$

It is well known [23] that the response $\mathbf{x}(t)$ for given parameters **a** is a Gaussian process with zero mean, spectral density

$$S_x^{(j,l)}(\omega|\mathbf{a}) \simeq \sum_{r=1}^{N_m}\sum_{s=1}^{N_m}\phi_j^{(r)}\phi_l^{(s)} \times \frac{S_{f0}^{(r,s)}}{[(\omega_r^2-\omega^2)+2\mathrm{i}\omega\omega_r\zeta_r][(\omega_s^2-\omega^2)-2\mathrm{i}\omega\omega_s\zeta_s]} \tag{17}$$

and correlation function

$$R_x^{(j,l)}(\tau|\mathbf{a}) = \int_{-\infty}^{\infty} S_x^{(j,l)}(\omega|\mathbf{a})\,\mathrm{e}^{\mathrm{i}\omega\tau}\,\mathrm{d}\omega \tag{18}$$

Assume that discrete data are available at $N_s(\leq N_d)$ measured DOFs. Also, assume that due to measurement noise and modeling error, there is prediction error, i.e. a difference between the measured response $\mathbf{y}(k) \in R^{N_s}$ and the model response corresponding to the measured degrees of freedom. The latter is given by $\mathbf{L}_0\mathbf{x}(k)$ where $\mathbf{L}_0$ is an $N_s \times N_d$ observation matrix, comprised of zeros and ones. That is,

$$\mathbf{y}(k) = \mathbf{L}_0\mathbf{x}(k) + \mathbf{n}(k) \tag{19}$$

It is assumed that the prediction error can be adequately represented by discrete zero-mean Gaussian white noise $\mathbf{n}(k) \in R^{N_s}$ with the following $N_s \times N_s$ covariance matrix:

$$E[\mathbf{n}(m)\mathbf{n}^{\mathrm{T}}(p)] = \mathbf{\Sigma}_n\delta_{m,p} \tag{20}$$

where $\delta_{m,p}$ is given by Eq. (7).

Here, we assume that only the lower N_m modes contribute significantly to the response and we will identify only the modal parameters corresponding to these modes. Specifically, the parameter vector **a** for identification is comprised of: (1) ω_r, ζ_r, $r = 1,\ldots,N_m$; (2) the elements of the first N_m columns of the $N_s \times N_d$ matrix $\mathbf{L}_0\mathbf{\Phi}$, excluding the elements used for the normalization of the modeshapes (which are fixed at unity); thus, a total of $N_m(N_s - 1)$ unknown modeshape parameters are to be identified; (3) the elements of the upper right triangular part of the $N_m \times N_m$ submatrix of $\mathbf{S}_{f0}$ corresponding to the N_m considered modes (symmetry defines the lower triangular part); (4) the elements of the upper right triangular part of $\mathbf{\Sigma}_n$ (again, symmetry defines the lower triangular part of this matrix).

Recall that the scaling of each modeshape is chosen such that one of its components corresponding to a measured DOF is equal to unity. However, such scaling is arbitrary. Thus, the above vectors can be identified only up to a constant scaling factor. A different modeshape normalization will cause all identified components of the rth modeshape to be scaled by some constant c_r; at the same time, the values of the elements $S_{f0}^{(r,s)}$ of the modal forcing spectral density matrix will be scaled by $(c_r c_s)^{-1}$.

Let the vector $\mathbf{Y}_{m,p}$ denote the response measurements from time $m\Delta t$ to $p\Delta t$ $(m \leq p)$, that is,

$$\mathbf{Y}_{m,p} = [\mathbf{y}^{\mathrm{T}}(m)\cdots\mathbf{y}^{\mathrm{T}}(p)]^{\mathrm{T}}, \qquad m \leq p \tag{21}$$

Using Bayes' theorem, the expression for the updated

PDF of the parameters $\mathbf{a}$ given some measured response $\mathbf{Y}_{1,N}$ is

$$p(\mathbf{a}|\mathbf{Y}_{1,N}) = c_2 p(\mathbf{a}) p(\mathbf{Y}_{1,N}|\mathbf{a}) \tag{22}$$

where c_2 is a normalizing constant such that the integral of the right-hand side of Eq. (22) over the domain of $\mathbf{a}$ is equal to unity. The term $p(\mathbf{a})$ denotes the prior PDF of the parameters and is based on previous knowledge or engineering judgement; in the case where no prior information is available, this term is treated as a constant. The term $p(\mathbf{Y}_{1,N}|\mathbf{a})$ is the dominant term on the right-hand side of Eq. (22) reflecting the contribution of the measured data in establishing the updated distribution. This term can be expanded into a product of conditional probabilities as follows:

$$p(\mathbf{Y}_{1,N}|\mathbf{a}) = p(\mathbf{Y}_{1,N_p}|\mathbf{a}) \prod_{k=N_p+1}^{N} p(\mathbf{y}(k)|\mathbf{a}; \mathbf{Y}_{1,k-1}) \tag{23}$$

In order to improve computational efficiency, the following approximation is introduced:

$$p(\mathbf{Y}_{1,N}|\mathbf{a}) \simeq p(\mathbf{Y}_{1,N_p}|\mathbf{a}) \prod_{k=N_p+1}^{N} p(\mathbf{y}(k)|\mathbf{a}; \mathbf{Y}_{k-N_p,k-1}) \tag{24}$$

That is, the conditional probability terms depending on more than N_p previous data points are approximated by conditional probabilities depending on only the last N_p data points. The sense of this approximation is that data points belonging too far in the past do not have a significant effect on the statistical behavior of a present point. Of course, one expects that this is true when N_p is so large that all the correlation functions have decayed to very small values. However, it will be shown with a numerical example later in Section 3.1 that a significantly smaller value of N_p suffices for the approximation in Eq. (24) to be valid for practical purposes. In particular, it is found that a value for N_p of the order of $T_0/\Delta t$ is sufficient, where T_0 is the fundamental period of the system and Δt the sampling time step. For example, assuming a time step $\Delta t = (1/25)T_0$, it follows that a value of $N_p \approx 25$ is sufficient. The advantage of the approximation in Eq. (24) will become obvious later in this section once the expression for the involved conditional probabilities is given.

The term $p(\mathbf{Y}_{1,N_p}|\mathbf{a})$ follows an N_sN_p-variate Gaussian distribution with zero mean and covariance matrix $\mathbf{\Sigma}_{Y,N_p}$:

$$\mathbf{\Sigma}_{Y,N_p} = E[\mathbf{Y}_{1,N_p}\mathbf{Y}_{1,N_p}^{\mathrm{T}}] = \begin{bmatrix} \mathbf{A}_{1,1} & \cdots & \mathbf{A}_{1,N_p} \\ \vdots & \ddots & \vdots \\ \mathbf{A}_{N_p,1} & \cdots & \mathbf{A}_{N_p,N_p} \end{bmatrix} \tag{25}$$

where each of the matrices $\mathbf{A}_{m,p}$, $1 \le m,\ p \le N_p$, has dimension $N_s \times N_s$. The $(j,\ l)$ element of the matrix $\mathbf{A}_{m,p}$ is given by

$$A_{m,p}^{(j,l)} = E[y_j(t + m\Delta t) y_l(t + p\Delta t)]$$

$$= \sum_{r,s=1}^{N_s} L_0^{(j,r)} L_0^{(l,s)} R_x^{(r,s)}[(p-m)\Delta t] + \Sigma_n^{(j,l)} \delta_{m,p} \tag{26}$$

where $\delta_{m,p}$ is the Kronecker delta function, $R_x^{(r,s)}$ the $(r,\ s)$ element of the auto-correlation function $\mathbf{R}_x(t)$ of the model response $\mathbf{x}(t)$ given by Eq. (18), and $\Sigma_n^{(j,l)}$ is the $(j,\ l)$ element of the noise covariance matrix defined in Eq. (20). It is worth noting that all matrices $\mathbf{A}_{m,p}$ with the same value of $(m-p)$ are identical and that $A_{m,p}^{(j,l)} = A_{p,m}^{(l,j)}$.

Thus, the joint probability distribution $p(\mathbf{Y}_{1,N_p}|\mathbf{a})$ is given by

$$p(\mathbf{Y}_{1,N_p}|\mathbf{a}) = \frac{1}{(2\pi)^{N_sN_p/2}|\mathbf{\Sigma}_{Y,N_p}|^{1/2}} \exp\left(-\frac{1}{2}\mathbf{Y}_{1,N_p}^{\mathrm{T}} \mathbf{\Sigma}_{Y,N_p}^{-1} \mathbf{Y}_{1,N_p}\right) \tag{27}$$

Next, we derive the general expression for the conditional probability of $\mathbf{y}(k)$ given α previous points $p(\mathbf{y}(k)|\mathbf{a}; \mathbf{Y}_{k-\alpha,k-1})$, where it is assumed that $k > \alpha \ge 1$. Note that the terms in the product of the right-hand side of Eq. (24) correspond to the special case $\alpha = N_p$. For notation simplicity in the later formulation, we introduce the vector $\mathbf{Z}(k) = [\mathbf{y}^{\mathrm{T}}(k)\ \mathbf{y}^{\mathrm{T}}(k-1)\cdots\mathbf{y}^{\mathrm{T}}(k-\alpha)]^{\mathrm{T}} \in \mathscr{R}^{N_s(\alpha+1)}$. Note that $\mathbf{Z}(k)$ is comprised of the same elements as the vector $\mathbf{Y}_{k-\alpha,k}$ in Eq. (21) but with the elements placed in reverse order. It can be calculated as follows:

$$\mathbf{Z}(k) \equiv \mathbf{B}_{\alpha+1}\mathbf{Y}_{k-\alpha,k} = \begin{bmatrix} \mathbf{y}(k) \\ \mathbf{B}_\alpha \mathbf{Y}_{k-\alpha,k-1} \end{bmatrix} \tag{28}$$

where the matrix $\mathbf{B}_\alpha$ is given by

$$\mathbf{B}_\alpha = \begin{bmatrix} \mathbf{D}_{1,1}^{(\alpha)} & \cdots & \mathbf{D}_{1,\alpha}^{(\alpha)} \\ \vdots & \ddots & \vdots \\ \mathbf{D}_{\alpha,1}^{(\alpha)} & \cdots & \mathbf{D}_{\alpha,\alpha}^{(\alpha)} \end{bmatrix} \tag{29}$$

with each of the matrices $\mathbf{D}_{m,p}^{(\alpha)}$, $m,p = 1, \ldots, \alpha$, of dimension $N_s \times N_s$ given by

$$\mathbf{D}_{m,p}^{(\alpha)} = \mathbf{I}_{N_s}\delta_{m+p,\alpha+1} \tag{30}$$

where $\mathbf{I}_{N_s}$ denotes the identity matrix of dimension $N_s \times N_s$ and $\delta_{m+p,\alpha+1}$ the Kronecker delta function. Since both the model response $\mathbf{x}$ and the prediction error $\mathbf{n}$ are zero-mean Gaussian processes, it follows from Eq. (19) that $\mathbf{y}$ is also a zero-mean Gaussian process. The covariance matrix $\mathbf{\Sigma}_Z$ of the random vector $\mathbf{Z}(k)$ is given by

$$\mathbf{\Sigma}_Z = E[\mathbf{Z}(k)\mathbf{Z}^{\mathrm{T}}(k)] = \begin{bmatrix} \mathbf{A}_{1,1}^{\mathrm{T}} & \cdots & \mathbf{A}_{1,\alpha+1}^{\mathrm{T}} \\ \vdots & \ddots & \vdots \\ \mathbf{A}_{\alpha+1,1}^{\mathrm{T}} & \cdots & \mathbf{A}_{\alpha+1,\alpha+1}^{\mathrm{T}} \end{bmatrix} \tag{31}$$

where each of the matrices $\mathbf{A}_{m,p}$, $1 \le m,p \le \alpha + 1$, is given

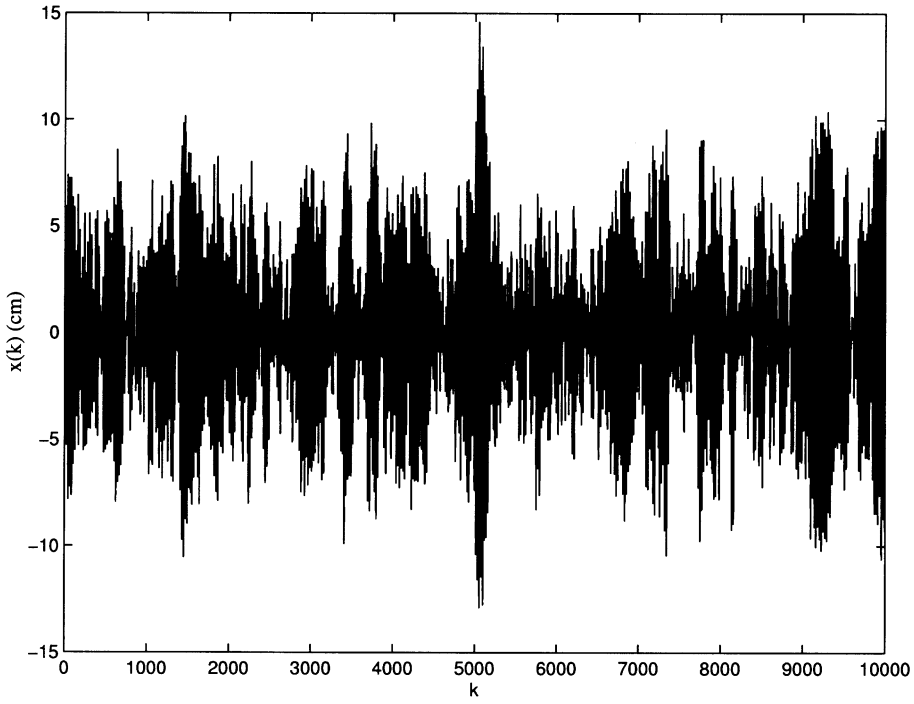

Fig. 1. Measured response (displ.) time history (Example 1).

by Eq. (26). Note that we take transpose of each of the matrices $\mathbf{A}_{m,p}$, $1 \le m$, $p \le \alpha + 1$ because the time order of the response vector was reversed.

Next, we partition the matrix $\mathbf{\Sigma}_Z$ as follows:

$$\mathbf{\Sigma}_Z = \begin{bmatrix} \mathbf{\Sigma}_{11} & \mathbf{\Sigma}_{12} \\ \mathbf{\Sigma}_{12}^{\mathrm{T}} & \mathbf{\Sigma}_{22} \end{bmatrix} \tag{32}$$

where $\mathbf{\Sigma}_{11}$, $\mathbf{\Sigma}_{12}$ and $\mathbf{\Sigma}_{22}$ have dimensions $N_s \times N_s$, $N_s \times N_s\alpha$ and $N_s\alpha \times N_s\alpha$, respectively. Since the measured response is assumed to have zero mean, the mean $\mathbf{e}_\alpha(k)$ of $\mathbf{y}(k)$ given $\mathbf{Y}_{k-\alpha,k-1}$ $(k > \alpha)$ is given according to Ref. [24] by

$$\mathbf{e}_\alpha(k) \equiv E[\mathbf{y}(k)|\mathbf{Y}_{k-\alpha,k-1}] = \mathbf{\Sigma}_{12}\mathbf{\Sigma}_{22}^{-1}\mathbf{B}_\alpha\mathbf{Y}_{k-\alpha,k-1} \tag{33}$$

and the covariance matrix $\mathbf{\Sigma}_{\epsilon,\alpha}(k)$ of the prediction error $\boldsymbol{\epsilon}_\alpha(k) = \mathbf{y}(k) - \mathbf{e}_\alpha(k)$ given $\mathbf{Y}_{k-\alpha,k-1}$ is given by

$$\mathbf{\Sigma}_{\epsilon,\alpha}(k) \equiv E[\boldsymbol{\epsilon}_\alpha(k)\boldsymbol{\epsilon}_\alpha^{\mathrm{T}}(k)] = \mathbf{\Sigma}_{11} - \mathbf{\Sigma}_{12}\mathbf{\Sigma}_{22}^{-1}\mathbf{\Sigma}_{12}^{\mathrm{T}} \tag{34}$$

It is worth noting that $\mathbf{\Sigma}_{\epsilon,\alpha}(k)$ is independent of the value of k. That is, $\mathbf{\Sigma}_{\epsilon,\alpha}(k) \equiv \mathbf{\Sigma}_{\epsilon,\alpha}$. In conclusion, the conditional probability $p(\mathbf{y}(k)|\mathbf{a}; \mathbf{Y}_{k-\alpha,k-1})$ follows an N_s-variate Gaussian distribution with mean $\mathbf{e}_\alpha(k)$ given by Eq. (33) and covariance matrix $\mathbf{\Sigma}_{\epsilon,\alpha}$ given by Eq. (34), that is,

$$p(\mathbf{y}(k)|\mathbf{a}; \mathbf{Y}_{k-\alpha,k-1}) = \frac{1}{(2\pi)^{N_s/2}|\mathbf{\Sigma}_{\epsilon,\alpha}|^{1/2}} \times \exp\left\{-\frac{1}{2}[\mathbf{y}(k) - \mathbf{e}_\alpha(k)]^{\mathrm{T}}\mathbf{\Sigma}_{\epsilon,\alpha}^{-1}[\mathbf{y}(k) - \mathbf{e}_\alpha(k)]\right\} \tag{35}$$

The proposed modal updating approach can be summarized as follows: We use Eq. (22) with $p(\mathbf{Y}_{1,N}|\mathbf{a})$ being calculated through the approximation in Eq. (24). The term $p(\mathbf{Y}_{1,N_p}|\mathbf{a})$ in Eq. (24) can be calculated using Eq. (27) along with Eqs. (25) and (26) and each of the remaining conditional probability terms in approximation (24) can be calculated with the help of Eq. (35) along with Eqs. (29)–(34).

One of the advantages of the approximation introduced in Eq. (24) is that all the conditional probability terms on the right-hand side are conditional on exactly N_p previous points. Thus, they follow an N_s-variate Gaussian distribution with the same covariance matrix $\mathbf{\Sigma}_{\epsilon,N_p}$ which, therefore, needs to be calculated only once. Also, the matrix $\mathbf{\Sigma}_{12}\mathbf{\Sigma}_{22}^{-1}$ in Eq. (33) for calculating the mean value of each of these distributions needs to be calculated only once for all these terms. Another major advantage is that one needs to calculate the inverse and determinant only for the matrices $\mathbf{\Sigma}_{Y,N_p}$, $\mathbf{\Sigma}_{22}$ and $\mathbf{\Sigma}_{\epsilon,N_p}$, of dimension $N_sN_p \times N_sN_p$, $N_sN_p \times N_sN_p$ and $N_s \times N_s$, respectively. This effort is negligible compared to the effort required in an exact formulation where one needs to calculate the inverse and the determinant of a matrix of dimension $N_sN \times N_sN$ (where generally $N \gg N_p$).

The most probable parameters $\hat{\mathbf{a}}$, also referred to as 'optimal', are obtained by minimizing $g(\mathbf{a}) = -\ln[p(\mathbf{a}|\mathbf{Y}_{1,N})]$. It is found that the updated PDF of the parameters $\mathbf{a}$ can be well approximated by a Gaussian distribution $N(\hat{\mathbf{a}}, \mathbf{H}^{-1}(\hat{\mathbf{a}}))$ with mean $\hat{\mathbf{a}}$ and covariance matrix $\mathbf{H}^{-1}(\hat{\mathbf{a}})$, where $\mathbf{H}(\hat{\mathbf{a}})$ denotes the Hessian of $g(\mathbf{a})$ calculated at $\mathbf{a} = \hat{\mathbf{a}}$.

Although the above formulation was presented for the case where the measured response is assumed to consist

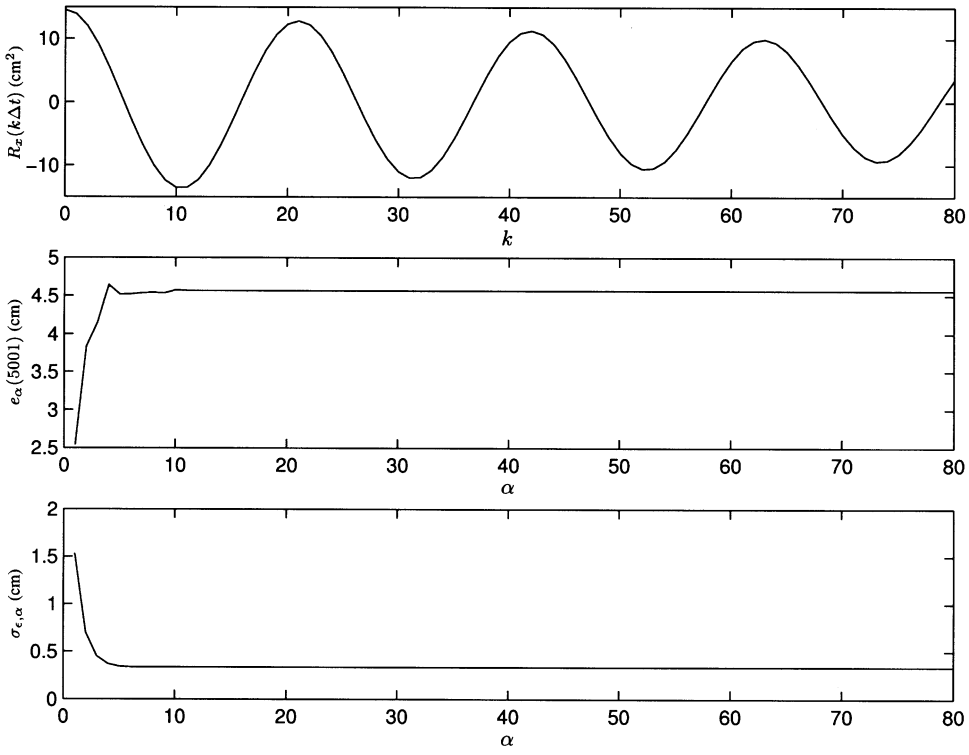

Fig. 2. Auto-correlation function R_x, mean predictive response e_α, and standard deviation of the predition error $\sigma_{\epsilon,\alpha}$ ($\Delta t = 0.1$ sec) (Example 1).

of displacement histories, it can be easily modified to treat velocity or acceleration measurements. In such a case, one must simply employ in the right-hand side of Eq. (17) the corresponding expressions for velocity or acceleration. Also, note that in the case of accelerations, one must assume band limited white noise in order to achieve bounded auto-correlation functions.

Note that in both the Kalman filter method and in the proposed approach, the response at a given time $k\Delta t$ is estimated using previous response measurements. However, in contrast to the Kalman Filter where the estimation is based on all available previous response measurements, the proposed approach utilizes only a limited number of the most recent N_p previous measurements. Moreover, in the case of Kalman filter, the estimators are calculated in a recursive manner; specifically, the predictor at time $k\Delta t$ can be calculated only after the predictor at time $(k-1)\Delta t$ becomes available. However, in the proposed approach, the predictor at any time $k\Delta t$ can be calculated directly from the last N_p measurements without the need to pre-calculate the predictor at any previous time. This allows for a computationally very efficient implementation of the proposed method when parallel computing is available.

Table 1
Identification results using one set of response data (Example 1)

Parameter	Actual $\tilde{\mathbf{a}}$	Optimal $\hat{\mathbf{a}}$	S.D. of σ	$\alpha = \sigma/\tilde{\mathbf{a}}$	$\beta = \lvert\tilde{\mathbf{a}} - \hat{\mathbf{a}}\rvert/\sigma$
ω_0	3.0000	3.0052	0.0079	0.0026	0.6599
ζ	0.0200	0.0203	0.0027	0.1342	0.0945
S_{f0}	5.0000	4.8413	0.1598	0.0320	0.9934
σ_n^2	0.1381	0.1396	0.0025	0.0183	0.6182

3. Numerical examples

3.1. Example 1 (SDOF)

In this example, we consider the identification of an SDOF system from simulated noisy displacement response data. The parameters $\tilde{\mathbf{a}} = [\tilde{\omega}_0, \tilde{\zeta}, \tilde{S}_{f0}, \tilde{\sigma}_n^2]^{\mathrm{T}}$ used to generate the simulated data are: $\tilde{\omega}_0 = 3$ rad/s, $\tilde{\zeta} = 0.02$, $\tilde{S}_{f0} = 5\ \mathrm{cm}^2\ \mathrm{s}^{-3}$ and $\tilde{\sigma}_n^2 = 0.1381\ \mathrm{cm}^2$. The chosen value of $\tilde{\sigma}_n^2$ corresponds to a 10% prediction error level, i.e. the rms of the noise is 10% of the rms of the noise-free response. The sampling time step is $\Delta t = 0.1$ s, and the total time interval is $T = 1000$ s, i.e. $N = 10\,000$. In both Examples 1 and 2, a noninformative prior distribution $p(\mathbf{a})$ is assumed.

Fig. 1 shows a typical simulated displacement time history. Fig. 2 validates the approximation in Eq. (24). The top plot shows the auto-correlation function $R_x(k\Delta t|\tilde{\mathbf{a}})$ corresponding to the target parameters plotted against k. The mean $\mathbf{e}_\alpha(5001)$ calculated from Eq. (33) and the corresponding standard deviation of the prediction error $\sigma_{\epsilon,\alpha}$ calculated from Eq. (34) are shown in the middle and bottom plot, respectively, as a function of the number of previous points α considered. It can be clearly seen that for values of α beyond approximately $\alpha = 10$ (corresponding to only about

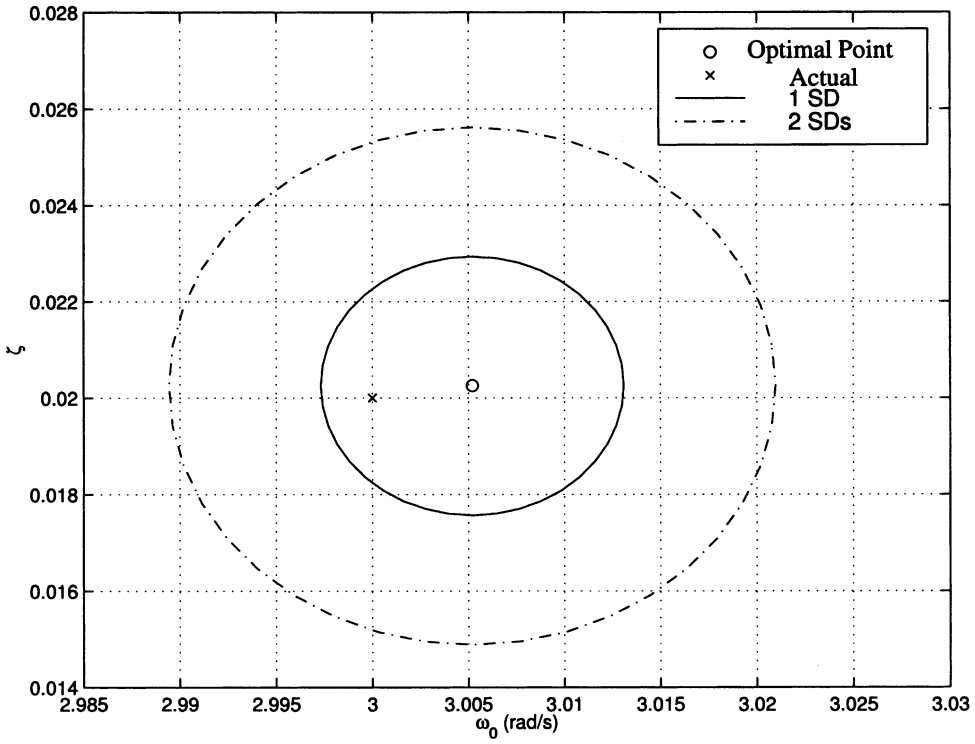

Fig. 3. Conditional updated joint PDF of frequency ω_0 and damping ratio ζ (Example 1).

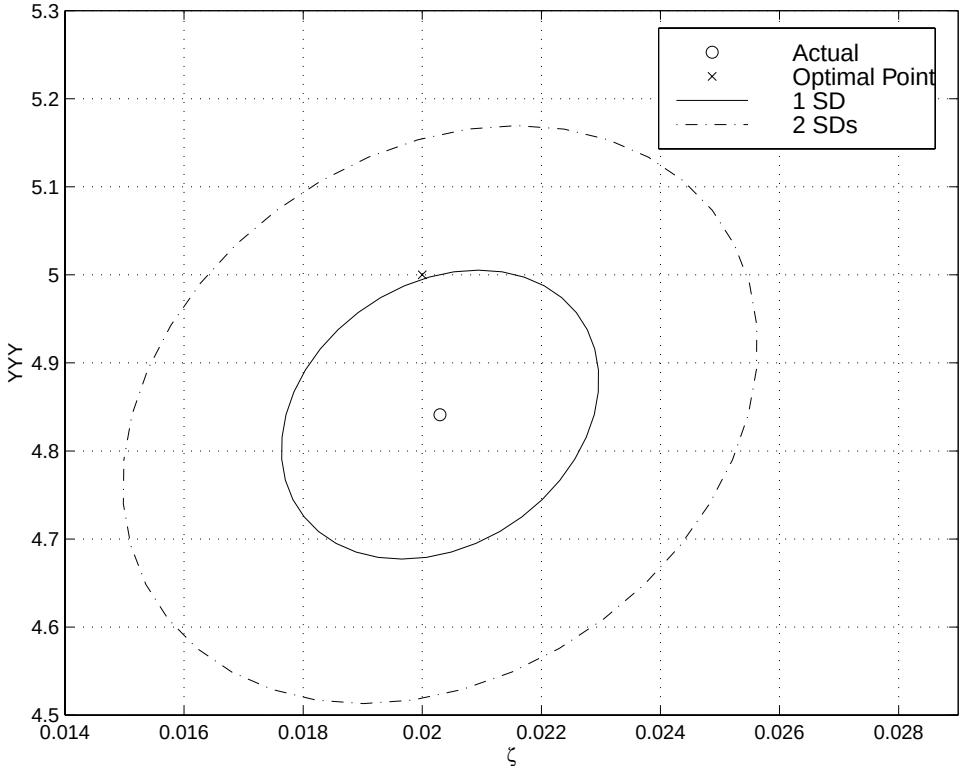

Fig. 4. Conditional updated joint PDF of damping ratio ζ and the spectral intensity $S_{f\,0}$ (Example 1).

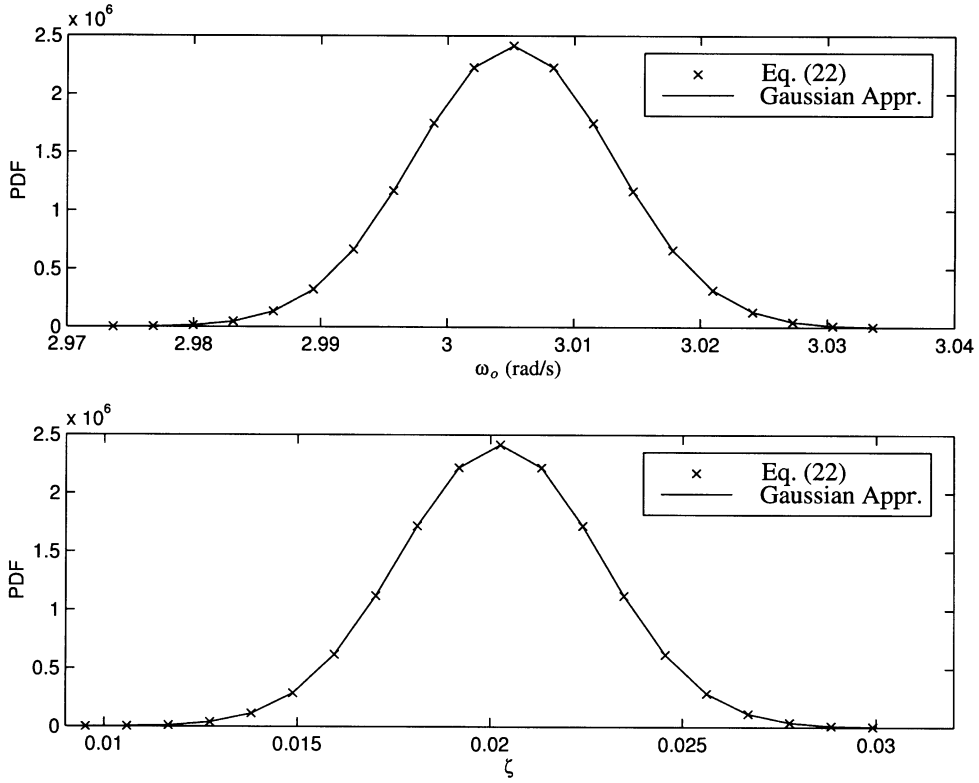

Fig. 5. Conditional PDFs of ω_0 and ζ calculated from: (i) Eqs. (22) and (24) - cross and (ii) Gaussian approximation - solid. The remaining parameters are fixed at their optimal values (Example 1).

one half of a period of the oscillator), the predictive response and its associated uncertainty stabilize. This implies that increasing the value of N_p beyond $N_p = 10$ in Eq. (24) will not further improve the quality of the identification results. Thus, it is suggested that N_p is chosen such that it contains approximately one period of the oscillator. It is worth noting that the value of N_p at which stabilization occurs is rather insensitive to the prediction error level (10% in our case). If one uses a larger value of N_p, the incremental improvement in the identification results will be insignificant but the computational effort will increase rapidly. The low value of N_p at which the values of $\mathbf{e}_\alpha$ and $\sigma_{\epsilon,\alpha}$ stabilize is rather surprising, given that the auto-correlation function is far from being decayed to small values. The computational efficiency of the presented algorithm is due to this low value of N_p.

Table 1 refers to the identification results using the single set of displacement measurements $\hat{\mathbf{Y}}_{1,N}$ shown in Fig. 1. It shows the estimated optimal values $\hat{\mathbf{a}} = [\hat{\omega}_0, \hat{\zeta}, \hat{S}_{f0}, \hat{\sigma}_n^2]^{\mathrm{T}}$,

Table 2
Identification results using 500 sets of data and $N_p = 20$ (Example 1)

Parameter	Actual $\tilde{\mathbf{a}}$	Average of $\hat{\mathbf{a}}$	S.D. of $\hat{\mathbf{a}}$	Average of σ	$E[\beta^2]$
ω_0	3.0000	2.9997	0.0074	0.0079	0.9300
ζ	0.0200	0.0205	0.0025	0.0027	0.9401
S_{f0}	5.0000	4.9892	0.1602	0.1646	0.9857
σ_n^2	0.1454	0.1454	0.0026	0.0025	1.0147

the calculated standard deviations $\sigma_{\omega 0}, \sigma_\zeta, \sigma_{S_{f0}}$ and $\sigma_{\sigma_n^2}$, the coefficient of variation (COV) for each parameter and the value of a 'normalized distance' β for each parameter. The parameter β represents the absolute value of the difference between the identified optimal and target value, normalized with respect to the corresponding calculated standard deviation. Here, the value $N_p = 20$ (corresponding to one period of the oscillator) was used in Eq. (24). Repeating the identification with a value of $N_p = 50$ yielded identical results.

Fig. 3 shows contours in the (ω_0, ζ) plane of the conditional updated joint PDF $p(\omega_0, \zeta|\hat{\mathbf{Y}}_{1,N}, \hat{S}_{f0}, \hat{\sigma}_n^2)$ calculated for the set of simulated data used in Table 1. Similarly, Fig. 4 shows contours in the (ζ, S_{f0}) plane of the conditional updated joint PDF $p(\zeta, S_{f0}|\hat{\mathbf{Y}}_{1,N}, \hat{\omega}_0, \hat{\sigma}_n^2)$ calculated for the same data. One observes that the damping ratio and the spectral intensity are quite correlated, in contrast to ω_0 and ζ which (as seen from Fig. 3) can be considered as being uncorrelated.

Fig. 5 shows conditional PDFs $p(\omega_0|\hat{\mathbf{Y}}_{1,N}, \hat{\zeta}, \hat{S}_{f0}, \hat{\sigma}_n^2)$ and $p(\zeta|\hat{\mathbf{Y}}_{1,N}, \hat{\omega}_0, \hat{S}_{f0}, \hat{\sigma}_n^2)$, obtained from: (i) Eqs. (22) and (24) (crosses) and (ii) the Gaussian approximation $N(\hat{\mathbf{a}}, \mathbf{H}^{-1}(\hat{\mathbf{a}}))$ described towards the end of Section 2.2 (solid line). It can be seen that the proposed Gaussian approximation is very accurate.

Next, 500 independent time history samples were generated, using the same parameters as discussed in the beginning of this example. The optimal parameters

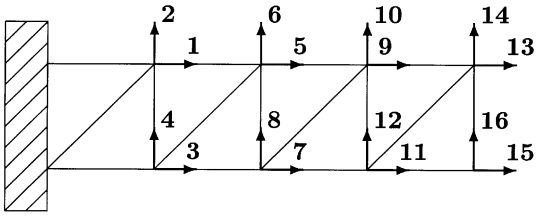

Fig. 6. Truss Model (Example 2).

$\hat{\mathbf{a}}^{(m)}, m = 1,\ldots,500$ using each set of data separately were calculated. Then, the mean value and the covariance matrix of the optimal parameters were calculated from the set $\{\hat{\mathbf{a}}^{(m)}, m = 1,\ldots,500\}$. The obtained mean values and standard deviations of the optimal parameters are shown in the third and fourth columns, respectively, of Table 2. The fifth column in this table shows the mean value of the 500 different standard deviations obtained by considering each of the above sets of data separately. Finally, the values of the second moments of the normalized distance parameter β, described earlier for Table 1, are shown in the last column. It can be seen that the fourth and the fifth columns look similar, implying that the uncertainties calculated from a single sample are representative of the uncertainties of the optimal parameters obtained from several independent sets of data of equal length. Furthermore, the values in the last column are all approximately equal to unity. This confirms that the calculated uncertainties from our proposed approach using one set of data are reasonable and representative of the true uncertainties in the identification process.

3.2. Example 2: four-bay truss

The second example refers to the truss shown in Fig. 6 where it is assumed that the displacements at the 8th, 12th and 15th DOFs were measured over a time interval $T = 2$ s, using a sampling interval $\Delta t = 1/2000$ s. The structure is assumed to be excited at all 16 DOFs with independent band-limited Gaussian white noise. The length of all the horizontal and vertical members is equal to 0.5 m. All members have the same cross-sectional area $A = 0.0004\ \mathrm{m}^2$. The mass density is $\rho = 7860\ \mathrm{kg/m}^3$ and the modulus of elasticity is $E = 200$ GPa. The first three modal frequencies are 87.2843, 299.2266 and 430.7872 Hz. The damping ratios are chosen to be 2% for all modes. The force excitations at the different DOFs are chosen to have identical spectral intensities equal to $1.0 \times 10^5\ \mathrm{N}^2\,\mathrm{s}$. The prediction error level is assumed to be 20%, i.e. the rms of the prediction error for a particular channel of measurement is equal to 20% of the rms of the noise-free response at the corresponding DOF. Identification using the proposed approach is carried out for the following four cases:

Case 1. Only response measurements from the 8th DOF are used to identify the lowest two modes.
Case 2. Only response measurements from the 12th DOF are used to identify the lowest two modes.
Case 3. Response measurements from the 8th and 15th DOFs are used to identify the lowest two modes.

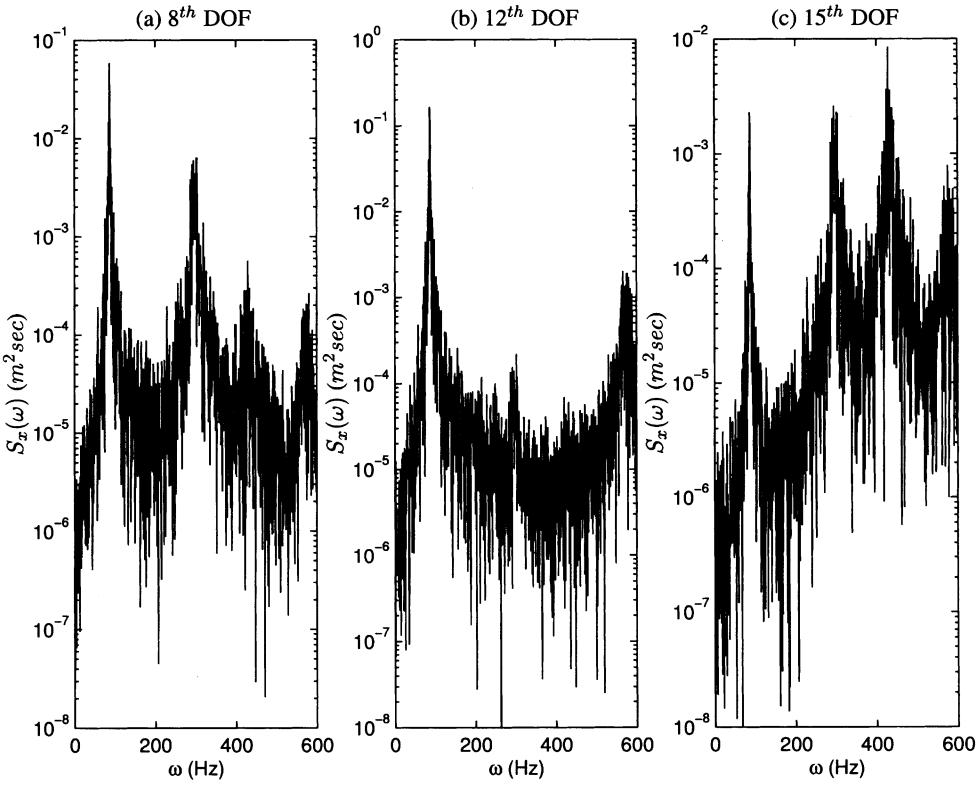

Fig. 7. Displacement spectral density for the 8^{th}, 12^{th} and 15^{th} DOF (Example 2).

Table 3
Identification results for Case 1 (Example 2)

Parameter	Actual $\tilde{\mathbf{a}}$	Optimal $\hat{\mathbf{a}}$	S.D. of σ	COV α	$\beta = \lvert\tilde{\mathbf{a}} - \hat{\mathbf{a}}\rvert/\sigma$
ω_1	87.2843	87.6616	0.4179	0.0048	0.9029
ω_2	299.2266	298.3806	0.9757	0.0033	0.8671
ζ_1	0.0200	0.0216	0.0048	0.2378	0.3361
ζ_2	0.0200	0.0238	0.0036	0.1783	1.0571
$S_{f0}^{(1,1)}$	727.0104	712.1315	48.7471	0.0671	0.3052
$\gamma_{f0}^{(1,2)}$	−0.1702	0.1566	0.1479	0.8692	2.2089
$S_{f0}^{(2,2)}$	1812.6129	1931.1583	231.3648	0.1276	0.5124
σ_n^2	0.0130×10^{-3}	0.0165×10^{-3}	0.0005×10^{-3}	0.0376	7.0847

Case 4. Response measurements from the 8th and 15th DOFs are used to identify the lowest three modes.

In all cases, a value of $N_p = 25$ was used which corresponds to data points covering just over one fundamental period.

Fig. 7a–c shows the auto-spectral density function corresponding to the 8th, 12th and 15th DOF, respectively, obtained from one set of data. One can see that the frequency content differs from one DOF to another. Therefore, one expects that the identification results obtained using measurements from different DOFs will vary.

Tables 3–6 show the identification results for Cases 1-4, respectively. The second column in these tables corresponds to the actual values used for generation of the simulated measurement data; the third and fourth columns correspond to the identified optimal parameters and the corresponding standard deviations, respectively; the fifth column lists the COV for each parameter; and the last column shows the normalized distance parameter β described in Example 1. The first group of rows in each table corresponds to modal frequencies, the next to modal damping ratios, the next to the corresponding modeshape components (Cases 3 and 4), the next to elements of the modal forcing spectral matrix $\mathbf{S}_{f0}$, and the last to elements of the prediction error covariance matrix $\mathbf{\Sigma}_n$. The off-diagonal elements of the matrix $\mathbf{S}_{f0}$ are here presented as coherence parameters $\gamma_{f0}^{(j,l)} \equiv S_{f0}^{(j,l)}/\sqrt{S_{f0}^{(j,j)} S_{f0}^{(l,l)}}$. Note that in Cases 1, 3 and 4, the normalization of the modeshapes is such that the modeshape component at the 8th DOF is equal to unity for each of the modes considered. In contrast, the normalization of the modeshapes in Case 2 was done with respect to the 12th DOF. Therefore, direct comparison of the values of the elements of $\mathbf{S}_{f0}$ for Case 2 and the corresponding values for any of the other cases is meaningless.

It is worth noting that in all cases the COV for the frequencies are smaller than those for the damping ratios, indicating that frequencies are identified better than dampings. An additional result observed, but not tabulated, is that the modal damping ratios were found to exhibit significant correlation with the corresponding modal forcing spectral intensities.

The calculated uncertainties shown in the above tables are in accordance with our expectations. For example, the standard deviation of ω_1 in Case 1 is similar to its value in Case 2 which is not surprising if one observes from Fig. 7 that the first modes in both cases are of similar magnitude. However, the standard deviation of ω_2 in Case 2 is more than six times its value in Case 1 which is also not surprising if one observes from Fig. 7 that the second mode does not show up as strongly at the 12th DOF (Case 2) as it does at the 8th DOF (Case 1).

Note that the use of additional channels usually improves the identification results, i.e. it usually reduces the uncertainties of the identified modal parameters. For example,

Table 4
Identification results for Case 2 (Example 2)

Parameter	Actual $\tilde{\mathbf{a}}$	Optimal $\hat{\mathbf{a}}$	S.D. of σ	COV α	$\beta = \lvert\tilde{\mathbf{a}} - \hat{\mathbf{a}}\rvert/\sigma$
ω_1	87.2843	87.4633	0.4056	0.0046	0.4414
ω_2	299.2266	303.1618	6.8132	0.0228	0.5776
ζ_1	0.0200	0.0215	0.0047	0.2368	0.3069
ζ_2	0.0200	0.0086	0.0266	1.3276	0.4291
$S_{f0}^{(1,1)}$	2042.7711	1984.5913	126.4076	0.0619	0.4603
$\gamma_{f0}^{(1,2)}$	−0.1702	0.0838	1.3818	8.1189	0.1838
$S_{f0}^{(2,2)}$	39.0641	24.9088	90.0589	2.3054	0.1572
σ_n^2	0.0340×10^{-3}	0.0383×10^{-3}	0.0010×10^{-3}	0.0305	4.1509

Table 5
Identification results for Case 3 (Example 2)

Parameter	Actual $\tilde{\mathbf{a}}$	Optimal $\hat{\mathbf{a}}$	S.D. of σ	COV α	$\beta = \lvert\tilde{\mathbf{a}} - \hat{\mathbf{a}}\rvert/\sigma$
ω_1	87.2843	87.2905	0.4083	0.0047	0.0152
ω_2	299.2266	299.7950	0.8479	0.0028	0.6704
ζ_1	0.0200	0.0207	0.0047	0.2325	0.1597
ζ_2	0.0200	0.0207	0.0029	0.1453	0.2260
$\phi_{15}^{(1)}$	0.1976	0.1956	0.0034	0.0173	0.6119
$\phi_{15}^{(2)}$	−0.6276	−0.6418	0.0194	0.0309	0.7296
$S_{f0}^{(1,1)}$	727.0104	704.6307	45.8801	0.0631	0.4878
$\gamma_{f0}^{(1,2)}$	−0.1702	−0.5602	0.1291	0.7586	3.0204
$S_{f0}^{(2,2)}$	1812.6129	1647.7563	155.1697	0.0856	1.0624
$\Sigma_n^{(1,1)}$	0.0130×10^{-3}	0.0164×10^{-3}	0.0004×10^{-3}	0.0345	7.5705
$\Sigma_n^{(1,2)}/\sqrt{\Sigma_n^{(1,1)}\Sigma_n^{(2,2)}}$	0	0.2070	0.0178	Inf	11.5990
$\Sigma_n^{(2,1)}$	0.0012×10^{-3}	0.0130×10^{-3}	0.0003×10^{-3}	0.2544	37.2781

comparing the tabulated results for Cases 1 and 3 one sees that the uncertainties in the modal frequencies and dampings of the first two modes in Case 3 are smaller than those in Case 1. It is likely, however, that placement of the second sensor at a different DOF can further reduce the uncertainties of the frequencies. A rational procedure for selecting the optimal locations has been developed [25,26]. It is based on using a statistical approach for modal updating, such as the one proposed herein, and involves the minimization of the information entropy of the estimated parameters which is a unique measure of their uncertainty.

Comparing Table 5 (Case 3) and Table 6 (Case 4), one sees that the consideration of the higher (third) mode does not have any substantial impact on the values of the optimal parameters and the standard deviations of the two lower modes. However, it can be observed that in both cases the identified values for the covariance of the prediction error are always larger than the theoretical values. This is because while all 16 modes contribute to the structural response, the identification has been restricted to a small number of the lower modes. The contribution of the higher modes on the lower frequency range has the effect of an equivalent artificial noise which causes the identified mean values of the prediction error covariance to be larger than the actual values used in the simulations. As we consider more modes, these errors become smaller, and the estimates of the prediction error covariance approach the theoretical values. The improvement as more modes are considered can be seen by

Table 6
Identification results for Case 4 (Example 2)

Parameter	Actual $\tilde{\mathbf{a}}$	Optimal $\hat{\mathbf{a}}$	S.D. of σ	COV α	$\beta = \lvert\tilde{\mathbf{a}} - \hat{\mathbf{a}}\rvert/\sigma$
ω_1	87.2843	87.6587	0.4107	0.0047	0.9117
ω_2	299.2266	298.4979	0.8122	0.0027	0.8972
ω_3	430.7872	431.9040	1.0089	0.0023	1.1070
ζ_1	0.0200	0.0207	0.0047	0.2326	0.1601
ζ_2	0.0200	0.0192	0.0027	0.1349	0.2834
ζ_3	0.0200	0.0177	0.0024	0.1191	0.9540
$\phi_{15}^{(1)}$	0.1976	0.1967	0.0026	0.0130	0.3550
$\phi_{15}^{(2)}$	−0.6276	−0.6299	0.0144	0.0229	0.1599
$\phi_{15}^{(3)}$	3.5313	3.0264	0.2541	0.0720	1.9866
$S_{f0}^{(1,1)}$	727.0104	705.8729	46.6130	0.0641	0.4535
$\gamma_{f0}^{(1,2)}$	−0.1702	−0.0399	0.1111	0.6526	1.1731
$\gamma_{f0}^{(1,3)}$	−0.0303	0.6190	0.2072	6.8485	3.1334
$S_{f0}^{(2,2)}$	1812.6129	1534.4846	132.4609	0.0731	2.0997
$\gamma_{f0}^{(2,3)}$	−0.0247	0.2047	0.0938	3.7980	2.4461
$S_{f0}^{(3,3)}$	178.4726	177.6544	33.4678	0.1875	0.0244
$\Sigma_n^{(1,1)}$	0.0130×10^{-3}	0.0157×10^{-3}	0.0004×10^{-3}	0.0346	5.9909
$\Sigma_n^{(1,2)}/\sqrt{\Sigma_n^{(1,1)}\Sigma_n^{(2,2)}}$	0	0.0305	0.0206	Inf	1.4811
$\Sigma_n^{(2,2)}$	0.0012×10^{-3}	0.0059×10^{-3}	0.0002×10^{-3}	0.1396	26.8422

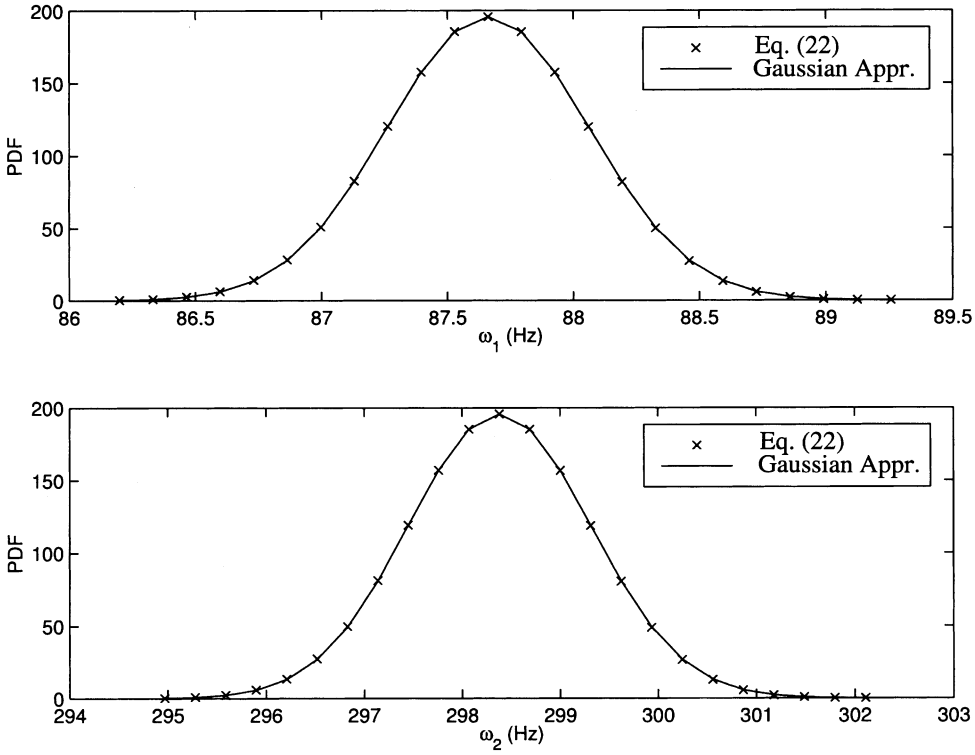

Fig. 8. Conditional PDFs of ω_1 and ω_2 for Case 1 calculated from: ω_1 (i) Eqs. (22) and (24) - cross; and (ii) Gaussian approximations - solid. The remaining parameters are fixed at their optimal values (Example 2).

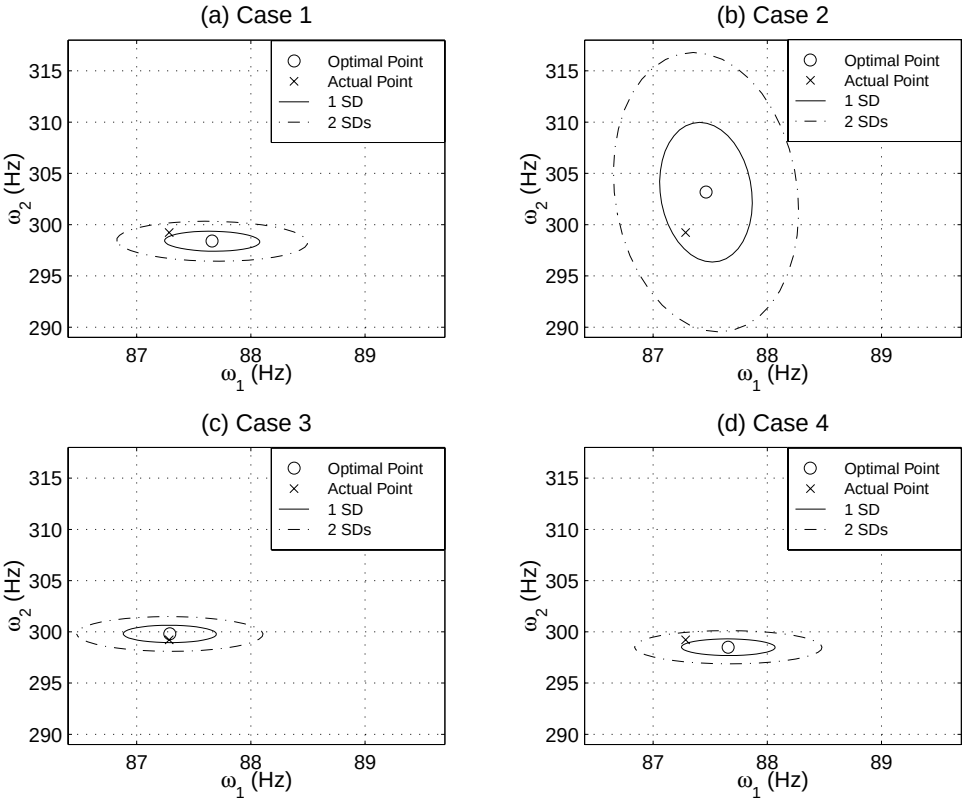

Fig. 9. Conditional updated joint PDF of natural frequencies ω_1 and ω_1 for Cases 1–4 (Example 2).

comparing Tables 5 and 6. Although in both Tables some of the identified elements of the prediction error covariance are far from the corresponding actual values, these discrepancies are relatively smaller in Case 4 (Table 6). It can be concluded that as more modes are considered this phenomenon of over-estimating the prediction error starts correcting itself.

Fig. 8 is a typical plot for Case 1 which shows conditional PDFs of ω_1 and ω_2 (keeping all other parameters fixed at their optimal values) obtained from: (i) Eqs. (22) and (24) (crosses) and (ii) the Gaussian approximation $N(\hat{\mathbf{a}}, \mathbf{H}^{-1}(\hat{\mathbf{a}}))$ described at the end of Section 2.2 (solid line). It can be seen that the proposed Gaussian approximation is very accurate.

Fig. 9a–d correspond to Cases 1–4, respectively, and show the contours in the (ω_1, ω_2) plane of the conditional updated joint PDF of ω_1 and ω_2 (keeping all other parameters fixed at their optimal values). One observes that in all cases the actual parameters are at a reasonable distance (measured in terms of the estimated standard deviations) from the identified optimal parameters. This, again, confirms that the calculated uncertainties are reasonable.

4. Concluding remarks

A Bayesian time–domain approach based on an approximate conditional probability expansion for updating the PDF of the modal parameters of a linear MDOF system using ambient data was presented. The updated PDF can be accurately approximated by a multi-variate Gaussian distribution. The calculated mean and covariance matrix of this distribution offer an estimate of the optimal values of the modal parameters and the uncertainties associated with these values. Calculation of the uncertainties of the identified modal parameters is very important if one plans to proceed in a subsequent step with the updating of a theoretical finite-element model.

The presented methodology processes simultaneously the response histories at all measured DOFs. Only one set of response time histories is required. The approach proceeds without any difficulty using directly the noisy measurement data. The calculation of the uncertainties does not require calculating several optimal values from a number of data sets and then calculating the statistics of these optimal estimates. Instead, it follows directly from the processing of a unique set of measurements. Note that the proposed methodology can be applied to the case of non-white stationary input by simply modifying Eqs. (11), (17) and (18) accordingly.

Acknowledgements

Financial support for this research from the Hong Kong Research Grant Council under grant HKUST 6041/97E and HKUST 6253/00E is gratefully acknowledged.

References

[1] Ewins DJ. Modal testing, theory and practice. New York: Wiley, 1995.
[2] Natke HG, Yao YPT. Proceedings of the Workshop on Structural Safety Evaluation Based on System Identification Approaches. Wiesbaden: Vieweg, 1988.
[3] Eykhoff P. System identification. New York: Wiley, 1974.
[4] Wright JR. Flutter test analysis in the time–domain using a recursive system representation. Journal of Aircraft 1974:774–7.
[5] Ibrahim SR. Double least squares approach for use in structural modal identification. AIAA Journal 1986;24(3):499–503.
[6] Pappa RS, Juang JN. Galileo spacecraft modal identification using an eigensystem realization algorithm. Journal of the Astronautical Sciences 1985;33(1):95–118.
[7] Golub GH, Van Loan CF. An analysis of total least squares problem. Journal of Numerical Analysis 1980;17(6):883–93.
[8] Cooper JE. Comparison of some time domain system identification techniques using approximate data correlations. International Journal of Analytical and Experimental Modal Analysis 1989;4:51–57.
[9] Asmussen JC, Ibrahim SR, Brincker R. Application of vector triggering random decrement. In: Proceedings of the 15th IMAC, vol. 2, Orlando, FL, 1997. p. 1165–71.
[10] Young PC. An instrumental variable method for real-time identification of a noisy process. Automatica 1970;6:271–87.
[11] Beck JL, Vanik MW, Polidori DC, May BS. Ambient vibration surveys of a steel frame building in a healthy and damaged state. Technical Report EERL 97-03. Pasadena (CA): California Institute of Technology, Earthquake Engineering Research Laboratory; 1997.
[12] Gersch W. Least squares estimates of structural system parameters using covariance function data. IEEE Transactions on Automatic Control 1974;19(6).
[13] Andersen P, Kirkergaard PH. Statistical damage detection of civil engineering structures using ARMAV models. In: Proceedings of the 16th IMAC, Santa Barbara, CA. 1998, p. 356–62.
[14] Goodwin GC, Sin KS. Adaptive filtering prediction and control. Englewood Cliffs, NJ: Prentice-Hall, 1984.
[15] Quek ST, Wang WP, Koh CG. System identification of linear MDOF structures under ambient excitation. Earthquake Engineering and Structural Dynamics 1999;28:61–77.
[16] Kalman RE. A new approach to linear filtering and prediction problems. Transactions of ASME, Journal of Basic Engineering 1960;82:35–45.
[17] Hoshiya M, Saito E. Structural identification by extended Kalman filter. Journal of Engineering Mechanics 1984;110(12):1757–70.
[18] Hoshiya M, Saito E. Estimation of dynamic properties of a multiple degrees of freedom linear system. In: Proceedings of the JSCE, vol. 344/I-1, 1984. p. 289–98.
[19] Hoshiya M. Application on extended Kalman filter-WGI method in dynamic system identification. Stochastic Structural Dynamics, Progress in Theory and Application 1988:103–24.
[20] Zeldin BA, Spanos PD. Spectral identification of nonlinear structural systems. Journal of Engineering Mechanics 1998;124(7):728–33.
[21] Beck JL, Katafygiotis LS. Updating models and their uncertainties. I: Bayesian statistical framework. Journal of Engineering Mechanics 1998;124(4):455–61.
[22] Katafygiotis LS, Papadimitriou C, Lam HF. A Probabilistic approach to structural model updating. Journal of Soil Dynamics and Earthquake Engineering 1998;17(7–8):495–507.
[23] Lutes LD, Sarkani S. Stochastic analysis of structural and mechanical vibrations. Englewood Cliffs, NJ: Prentice-Hall, 1997.
[24] Brockwell PJ, Davis RA. Time series: theory and methods. New York: Springer, 1991.
[25] Papadimitriou C, Beck JL, Au SK. Entropy-based optimal sensor location for structural model updating. Journal of Vibration and Control 2000;6(5):781–800.
[26] Katafygiotis LS, Papadimitriou C, Yuen KV. An optimal sensor location methodology for designing cost-effective modal experiments. In: Proceedings of the EURODYN'99, Prague, Czech Republic. 1999, p. 617–22.